J. Amr. Uni. ***01*** *(2021) p.129*

Dust Acoustic Multi-soliton Collisions in a Dusty Plasma Using Hirota Bilinear Method

Mahmood Ahmed Hassan Khaled[1,*], Mohamed Ali Shukri[2,†], and Yusra Abd-Ulrahman Hager[3,‡]
[1]Department of Physics, Faculty of Education, Sana'a University, Al-Mahweet, Yemen
[2] Department of Physics, Faculty of Science , Sana'a University, Sana'a, Yemen
[3] Department of Physics, Faculty of Education, Sana'a University, Sana'a, Yemen

Abstract

The propagation and collision of dust acoustic (DA) multi-solitons in a four component dusty plasma which consists of negatively and positively charged cold dust fluids, Boltzmann distributed electrons and ions have been studied in the presence of a polarization force acting on dust grains. Using the reductive perturbation technique (RPT), the Korteweged-de Vries (KdV) equation is derived. By using the Hirota bilinear method, the two-and three-soliton solutions of the obtained KdV equation have been successfully obtained. Phase shifts of the two-soliton and three-soliton have been deduced. It has been found that both compressive and rarefactive solitons exist in current dusty plasma model. The polarization force plays a significant role in the overtaking collision process of two-soliton and three-soliton, in such a way that the amplitude of the compressive (rarefactive) solitons decreases (increases) as polarization force increases. It was also found that the phase shifts are significantly affected by the dusty plasma parameters such as the dust charge number ratio, ion-to-electron temperature ratio, negative-to-positive dust mass ratio, the ratio of the densities of electrons to ions and the polarization force parameter.

Keywords: Multi-soliton collisions, KdV equation, polarization force, Phase shift.

الملخص: تم في هذه البحث دراسة انتشار وتصادم السوليتونات الصوتية الغبارية في بلازما غبارية مكونة من حبيبات غبار سالبة الشحنة وأخرى موجبة الشحنة والكترونات وايونات حرارية (تتبع توزيع بولتزمان) وذلك في وجود تأثير قوة الاستقطاب على حبيبات الغبار السالبة والموجبة. تم استخدام تقنية الاضطراب المختزلة لاشتقاق معادلة كورتيفيك–دي فريس (Korteweged–de Vries (KdV) equation). تم إيجاد الحلول متعددة السوليتونات لهذه المعادلة باستخدام نظرية Hirota bilinear . تم استنتاج إزاحات الطور الناتجة من تصادم الاجتياز بين سوليتونين وثلاثة سوليتونات متحركة بسرعات مختلفة. من خلال الدراسة وجدنا أن هناك نوعين من السوليتونات (تضاغطية وتخلخليه) وأن قوة الاستقطاب لها دور رئيسي في عمليات تصادم الاجتياز بين السوليتونات سواء كانت تضاغطية أو تخلخليه بحيث تقلل من سعة السوليتونات التضاغطية وتزيد من سعة السوليتونات التخلخليه. أيضا وجدنا أن إزاحة الطور تتأثر بشكل ملحوظ بواسطة بارامترات البلازما مثل نسبة عدد شحنات الغبار الموجب إلى السالب، نسبة كثافة الالكترونات إلى الايونات، نسبة درجة حرارة الايون إلى الإلكترون، نسبة كتلة حبيبة الغبار السالبة إلى الموجبة وبارامتر الاستقطاب.

1. Introduction

Nowadays, dusty plasma physics covers a wide spectrum of applications because of its importance in industrial plasma applications, in laboratory plasmas as well as astrophysical plasmas [1-4]. A dusty plasma is an usual electron-ion plasma with an additional charged component of massive dust grains [5]. The dynamics of dusty plasmas is very different from that of the usual electron-ion plasma. The existence of the charged dust grains in plasma can modify the collective behaviour of a plasma, as well as excite new modes and new nonlinear phenomena, such as dust ions acoustic waves [6] and dust acoustic waves [7, 8]. The dust acoustic (DA) wave is a very low frequency, longitudinal wave in which the wave is supported by the inertia of the dust grains, with the restoring force being provided by the pressure of both the electrons and ions. It is a sound wave

*E-mail: mahkhaled@hotmail.com
†E-mail: mshukri2006@gmail.com
‡E-mail: hager22013@gmail.com

propagating through the charged dust fluid, involving oscillations of the heavy dust grains. The existence of the DA wave was first theoretically investigated in the early 1990s by Rao, et al. [7], and later experimentally observed by Barkan et al. [8], who were able to produce fascinating images and real-time videos of the propagation of DA waves due to their low phase velocity and the large size of the dust grains.

It is important to note that the charged dust grains embedded in a plasma are subject to several forces acting on them. Probably, the most important one is the electrostatic force caused by separation of charges in the plasma. Another force acting on the dust grain is the polarization force which is due to the deformation of the Debye sheath around the dust grain in the background of non-uniform plasmas [9, 10]. Khrapak et al. [11] have investigated the effect of the polarization force on the propagation of the DA solitary waves. During the past years, a series of theoretical studies has been performed to investigate the propagation characteristics of the DA waves in the presence of the polarization force acting on dust grains in a background of non-uniform plasmas [12-16]. Most of these investigations have been published by assuming negatively charged massive dust grains due to the collection of electrons from background of plasma species. But there is direct evidence for the co-existence of both positively and negatively charged dust particles in different regions of space plasmas such as, the Earth's mesosphere [17], cometary tails [18], Jupiter's magnetospheres [19] and laboratory devices [20]. Recently, El-Taibany et al. [21] have studied the effects of polarization force on the electrostatic solitary waves. But they have ignored the effects of polarization force on the positive dust.

However, a dusty plasma medium with dispersive and nonlinearity properties, assists the formation of the associated nonlinear structures such as dust-acoustic solitary waves or solitons, which arise due to a balance between nonlinear effects and dispersion. Solitons are a particular type of solitary waves which maintain their shape and speed after interactions and have been extensively studied in mathematics and physics in the framework of the Korteweg-de Vries (KdV) equation.

Nowadays, solitons and their interactions are the most important nonlinear phenomenon in different plasma environments [22, 23]. Zabusky and Kruskal [24] numerically examined the nonlinear interaction of a large solitary-wave overtaking a smaller one. It was found that, after interaction, the solitary waves retained their original shapes, the only effect of the collision being a phase shift. Due to this special property, amongst others, the solitary-wave solution of the KdV equation is termed a soliton. Gardner et al. [25] showed that the KdV equation can be solved exactly using the inverse-scattering transform. Inverse scattering shows that the collision of the the KdV solitons is elastic, because the solitons retain their shapes after an interaction and no dispersive radiation is generated as a result of a collision. In addition, there is a very useful and efficient method for the determination of multiple soliton solutions of the KdV equation. This is known as the Hirota bilinear method [26]. It is a direct method to obtain exact solutions for a wide class of nonlinear evolution equations in the nonlinear science. Roy et al. [27] investigated the propagation of the ion acoustic two-soliton interaction in a three component collision-less unmagnetized plasma in the framework of the KdV equation. Applying the Hirota bilinear method, they derived two-soliton and corresponding phase shifts. Saha and Chatterjee [28] studied the propagation and interaction of the DA multi-soliton in a four component dusty plasma which consists of negatively and positively charged cold dust fluids, q-nonextensive electrons and ions. Using the Hirota bilinear method in the frameworks of the KdV equation, they obtained a two-soliton and three-soliton solutions of the KdV equation. They investigated corresponding phase shifts of the two-soliton and three-soliton as well. Recently, Khaled et al. [29] presented a theoretical model for the DA solitons in an opposite polarity dusty plasma system which consists of negatively and positively charged cold dust fluids, Boltzmann electrons and ions, including a generalized polarization force effect. They derived the KdV equation for this system by using the reductive perturbation method. Therefore in the present work, we extend the dusty plasma model of Khaled et al. [29] to study the overtaking collision and corresponding phase shifts of the DA two- soliton and three-soliton in the frameworks of the KdV equation by using the Hirota's bilinear method. We want to investigate the effects of the polarization force and the other dusty plasma parameters on the phase shifts and the formation of the two-soliton and three-soliton.

The paper is organized as follows: The theoretical model containing the basic equations governing our dusty plasma system is described in Sect. 2. In Sect.3, we obtain the KdV equation for our model. The multi-soliton solutions of the KdV equation are given in Sect. 4. In Sect. 5, we obtain the Behaviour of soliton collisions and phase shifts. Numerical results and discussion are presented in Sect.6. Sect. 7 is kept for conclusions.

2. Theoretical Method

We consider a collisionless, unmagnetized four-component dusty plasma consisting of negatively and positively charged cold dust fluids, and inertialess electrons and positive ions in the presence of a polarization force acting on massive charged dust grains. In a low frequency phenomena in the regime where dust dynamics is important, the inertia of the electrons and ions is assumed to be neglected and can be described by Boltzmann distribution. Thus, the number densities for electrons (n_e) and ions (n_i) can be given, respectively, by

$$n_e = n_{e0}\exp\left(\frac{e\varphi}{k_B T_e}\right), \tag{1}$$

$$n_i = n_{i0}\exp\left(-\frac{e\varphi}{k_B T_i}\right), \tag{2}$$

where $n_{e0}(n_{i0})$ is the equilibrium number density of electrons (ions), φ is the electrostatic potential. When the electrons and ions are considered to be Bolzmannian, the polarization force acting on a dust grain can be written as [9, 10]

$$\boldsymbol{F}_p = -\frac{Q_d^2}{8\pi\epsilon_0}\frac{\boldsymbol{\nabla}\lambda_D}{\lambda_D^2}, \tag{3}$$

where Q_d is the grain charge and λ_D is the linearized Debye radius and can be expressed as:

$$\lambda_D = \left[\frac{\epsilon_0 k_B T_i T_e}{e^2(n_i T_e + n_e T_i)}\right]^{1/2}. \tag{4}$$

Normalized λ_D by λ_{D0} and assuming that the potential perturbation is sufficiently small i.e., $\varphi \ll k_B T_e/e\,, k_B T_i/e$, we rewrite the linearized Debye radius λ_D as (see Ref. [29] for more details)

$$\lambda_D = \lambda_{D0}\left[1 - \alpha_1\left(\frac{e\varphi}{k_B T_i}\right) + \alpha_2\left(\frac{e\varphi}{k_B T_i}\right)^2\right]^{-1/2}, \tag{5}$$

where $\lambda_{D0} = [\epsilon_0 k_B T_i T_e/e^2(n_{i0}T_e + n_{e0}T_i)]^{1/2}$, $\alpha_1 = (1-\rho\sigma_i^2)/(1+\rho\sigma_i)$ and $\alpha_2 = (1+\rho\sigma_i^3)/2(1+\rho\sigma_i)$ with $\rho = n_{e0}/n_{i0}$ is the electron-to-ion number density ratio at equilibrium. Substituting Eq. (5) into Eq. (3), and after some algebraic calculations, we finally obtain the following expression of the polarization force [29]

$$\boldsymbol{F}_p = -eZ_d R\alpha_1\left(1 + P_0\frac{e\varphi}{k_B T_i}\right)\boldsymbol{\nabla}\varphi, \tag{6}$$

where $P_0 = (\alpha_1^2 - 4\alpha_2)/2\alpha_1$ and $R = Z_d e^2/16\pi\epsilon_0 k_B T_i \lambda_{D0}$ represent the effects of the polarization force. It is obvious from expression (6) that the polarization force is independent of the polarity of the dust grains, i.e. the polarization force will always be of the same nature whether the charge is positive or negative and it is always in the direction of decreasing Debye length.

Accordingly, the basic fluid equations (i.e. the continuity, the momentum and the Poisson equation) for negative and positive dust components, with the inclusion of the generalized polarization force in the dust momentum equations can be written as, respectively,

$$\frac{\partial n_n}{\partial t} + \frac{\partial}{\partial x}(n_n u_n) = 0, \tag{7}$$

$$\frac{\partial u_n}{\partial t} + u_n \frac{\partial u_n}{\partial x} = \frac{Z_n e}{m_n}\frac{\partial \varphi}{\partial x} - \frac{Z_n e}{m_n} P\left(1 + P_0 \frac{e\varphi}{k_B T_i}\right)\frac{\partial \varphi}{\partial x}, \tag{8}$$

$$\frac{\partial n_p}{\partial t} + \frac{\partial}{\partial x}\left(n_p u_p\right) = 0, \tag{9}$$

$$\frac{\partial u_p}{\partial T} + u_p \frac{\partial u_p}{\partial x} = -\frac{Z_p e}{m_p}\frac{\partial \phi}{\partial x} - \frac{Z_p e}{m_p} ZP\left(1 + P_0 \frac{e\varphi}{k_B T_i}\right)\frac{\partial \varphi}{\partial x}, \tag{10}$$

$$\frac{\partial^2 \varphi}{\partial x^2} = \frac{e}{\epsilon_0}\left(n_e + Z_n n_n - Z_p n_p - n_i\right), \tag{11}$$

where $n_n(n_p)$, $u_n(u_p)$, and $m_n(m_p)$ are the density, the velocity, and mass, of the negatively (positively) charged dust grains, respectively. Here $P = R\alpha_1$ and $Z = Z_p/Z_n$ is the ratio of positive-to-negative dust charge number with $Z_p(Z_n)$ is the number of charges residing on the positive (negative) dust grain surface. At equilibrium, the quasi-neutrality condition requires $Z_n n_{n0} + n_{e0} = Z_p n_{p0} + n_{i0}$, where n_{p0} (n_{n0}) is the equilibrium number density of positively (negatively) charged dust grains.

For notational clarity, we normalize the dynamic variables appearing in Eqs. (7)-(11) as follow: $N_n = n_n/n_{n0}$, $N_p = n_p/n_{p0}$, $U_n = u_n/C_{Dn}$, $U_p = u_p/C_{Dn}$ and $\phi = e\varphi/k_B T_i$ where $C_{dn} = (Z_n k_B T_i/m_n)^{1/2}$ being the sound speed of the negatively charged dust. The time t and space x variables are normalized as $T = t\omega_{pn}$ and $X = x/\lambda_{Dn}$where $\omega_{pn} = (n_{n0} Z_n^2 e^2/\epsilon_0 m_n)^{1/2}$ is the plasma frequency of the negatively charged dust and $\lambda_{Dn} = (\epsilon_0 k_B T_i/n_{n0} Z_n e^2)^{1/2}$ is Debye length of the negatively charged dust. Thus, Eqs. (7)-(11) becomes

$$\frac{\partial N_n}{\partial T} + \frac{\partial}{\partial X}(N_n U_n) = 0, \tag{12}$$

$$\frac{\partial U_n}{\partial T} + U_n \frac{\partial U_n}{\partial X} = \frac{\partial \phi}{\partial X} - P(1 + P_0 \phi)\frac{\partial \phi}{\partial X}, \tag{13}$$

$$\frac{\partial N_p}{\partial T} + \frac{\partial}{\partial X}\left(N_p U_p\right) = 0, \tag{14}$$

$$\frac{\partial U_p}{\partial T} + U_p \frac{\partial U_p}{\partial X} = -\mu Z \frac{\partial \phi}{\partial X} - \mu Z^2 P(1 + P_0 \phi)\frac{\partial \phi}{\partial X}, \tag{15}$$

$$\frac{\partial^2 \phi}{\partial X^2} = \mu_e \exp(\sigma_i \phi) - \mu_i \exp(-\phi) + N_n - \beta N_p\,, \tag{16}$$

where $\mu = m_n/m_p$, $\mu_e = n_{e0}/z_n n_{n0}$, $\mu_e = n_{e0}/z_n n_{n0}$ and $\beta = 1 + \mu_e - \mu_i$.

For simplicity, we may also expand the exponential functions in the normalized Poisson's equation (16) up to second order in ϕ. With using this expansion, Poisson's equation is simplified to

$$\frac{\partial^2 \phi}{\partial X^2} = (N_n - 1) + \beta\left(1 - N_p\right) + H_1 \phi + H_2 \phi^2 + \mathcal{O}(\phi^3), \tag{17}$$

where the coefficients H_1 and H_2 are calculated to be $H_1 = \mu_e \sigma_i + \mu_i$, and $H_2 = (\mu_e \sigma_i^2 - \mu_i)/2$.

3. Kortewg-De Vries (KdV) Equation

Since we are dealing with a weakly nonlinear theory for the small but finite amplitude DA waves, we employ the reductive perturbation method [30] to derive the K-dV equation. So, at first, we introduce the space and time stretched coordinates as

$$\xi = \epsilon^{1/2}(\mathrm{X} - V_0 T), \quad \tau = \epsilon^{3/2} T, \tag{18}$$

where ϵ is a smallness parameter characterizing the strength of the nonlinearity and V_0 is the normalized linear phase velocity of the DA wave. Then, we expand the dynamical quantities of the system about their equilibrium values in power series of ϵ as:

$$\Psi = \Psi^{(0)} + \epsilon\Psi^{(1)} + \epsilon^2\Psi^{(2)} + \cdots, \tag{19}$$

where $\Psi = (N_n,\ U_n,\ N_p,\ U_p,\ \phi)$ and $\Psi^{(0)} = (1,\ 0, 1, 0, 0)$.

Substituting equations (18) and (19) into equations (12)-(17) and collecting the terms in different powers of ϵ, we get the following equations for lowest order

$$N_n^{(1)} = \frac{U_n^{(1)}}{V_0} = -\frac{(1-P)}{V_0^2}\phi^{(1)}, \tag{20}$$

$$N_p^{(1)} = \frac{U_p^{(1)}}{V_0} = \frac{\mu Z(1+ZP)}{V_0^2}\phi^{(1)}, \tag{21}$$

$$N_n^{(1)} - \beta N_p^{(1)} + H_1\phi^{(1)} = 0. \tag{22}$$

From these equations we get the linear phase velocity relation of solitons as

$$V_0 = \sqrt{\frac{1+\mu Z\beta - P(1-\mu\beta Z^2)}{H_1}}. \tag{23}$$

It is obvious from Eq. (23) that the value of V_0 decreases with the increasing values of P i.e., the polarization force effect causes a decrease of the wave phase velocity. This effect becomes more and more important for larger dust grains**.**

The next-order in ϵ gives another set of coupled equations. Solving these equations with the aid of Eqs. (20)-(22), we finally obtain the well-known KdV equation as

$$\frac{\partial\phi^{(1)}}{\partial\tau} + A\,\phi^{(1)}\frac{\partial\phi^{(1)}}{\partial\xi} + B\frac{\partial^3\phi^{(1)}}{\partial\xi^3} = 0, \tag{24}$$

where the coefficients of nonlinearity (A) and dispersion (B) appearing in the K-dV equation are given by

$$A = \frac{1}{2H_1V_0^3}[3\beta\mu^2Z^2(1+ZP)^2 - 3(1-P)^2 + PP_0(\beta\mu Z^2 - 1)V_0^2 - 2H_2V_0^4],$$

and

$$B = \frac{V_0}{2H_1}.$$

4. Multi-Soliton Solutions of KdV Equation

In order to examine the collision of a multi-soliton in the framework of a KdV equation (24), we employ the Hirota bilinear method. We first use the transformation: $\xi = \zeta\sqrt[3]{B}$, $\phi^{(1)}(\xi,\tau) = 6\sqrt[3]{B}A^{-1}\psi(\zeta,\tau)$, and $\tau = \tau$ to convert the KdV equation.(24) to its standard form. Then we get

$$\frac{\partial\psi}{\partial\tau} + 6\,\psi\frac{\partial\psi}{\partial\zeta} + \frac{\partial^3\psi}{\partial\zeta^3} = 0. \tag{25}$$

Note that the standard KdV equation (25) can have multi-soliton solutions describing the dynamics of interactions (collisions) of the multi-soliton. The solution of the standard KdV equation (25) can be expressed by

$$\psi(\zeta,\tau) = 2\frac{\partial^2}{\partial\zeta^2}\ln F(\zeta,\tau) = 2\left(\frac{FF_{\zeta\zeta} - F_\zeta^2}{F^2}\right), \tag{26}$$

where the function $F(\zeta,\tau)$ is chosen to have a perturbation expansion form, defined as

$$F(\zeta,\tau) = 1 + \epsilon f_1(\zeta,\tau) + \epsilon^2 f_2(\zeta,\tau) + \epsilon^3 f_3(\zeta,\tau) + \cdots, \tag{27}$$

where ϵ is a non-small formal expansion parameter. The unknown functions $f_1(\zeta,\tau)$, $f_2(\zeta,\tau)$, ... can be determined later. Substituting Eq. (26) into a standard KdV equation (25), integrating once and setting the integration constant equal to zero, allows us to replace (25) by

$$FF_{\zeta\tau} - F_\zeta F_\tau + FF_{\zeta\zeta\zeta\zeta} - 4F_{\zeta\zeta\zeta}F_\zeta + 3F_{\zeta\zeta}^2 = 0. \tag{28}$$

This equation is a quadratic equation in $F(\zeta,\tau)$ (Hirota usually refers to this as a bilinear equation). Using the Hirota bilinear-D operator notation, equation (28) can be written as

$$\hat{B}(F.F) = \left(D_\zeta\, D_\tau + D_\zeta^4\right)(F.F) = 0. \tag{29}$$

In order to obtain the Multi-Soliton solutions of a KdV equation, we solve the bilinear equation of the KdV equation. Substituting Eq. (27) into Eq. (29) and equating to zero the powers of ε, yields

$$\boldsymbol{O(\epsilon^0)}: \qquad \boldsymbol{\hat{B}(1\cdot 1) = 0}, \tag{30a}$$

$$\boldsymbol{O(\epsilon^1)}: \qquad \boldsymbol{\hat{B}(1\cdot f_1 + f_1\cdot 1) = 0}, \tag{30b}$$

$$\boldsymbol{O(\epsilon^2)}: \qquad \boldsymbol{\hat{B}(1\cdot f_2 + f_1\cdot f_1 + f_2\cdot 1) = 0}, \tag{30c}$$

$$\boldsymbol{O(\epsilon^3)}: \qquad \boldsymbol{\hat{B}(1\cdot f_3 + f_1\cdot f_2 + f_2\cdot f_1 + f_3\cdot 1) = 0}, \tag{30d}$$

$$\vdots$$

$$\boldsymbol{O(\epsilon^n)}: \qquad \boldsymbol{\hat{B}\left(\sum_{m=0}^{n} f_m\cdot f_{n-m}\right) = 0}, \tag{30e}$$

where $f_0 = 1$, and $\hat{B} = D_\zeta\, D_\tau + D_\zeta^4$. From equation (30d) we obtain

$$\left(\frac{\partial^2}{\partial\zeta\partial\tau} + \frac{\partial^4}{\partial\zeta^4}\right)f_n = -\frac{1}{2}\sum_{m=1}^{n-1}\hat{B}(f_m\cdot f_{n-m}), \tag{31}$$

Equation (31) must be solved recursively to find $F(\zeta,\tau)$ with $n = 1, 2, 3, \ldots$.
From Eq. (31), when $n = 1$, $n = 2$, $n = 3$ we have

$$\left(\frac{\partial^2}{\partial\zeta\partial\tau} + \frac{\partial^4}{\partial\zeta^4}\right)f_1 = 0, \tag{32a}$$

$$\left(\frac{\partial^2}{\partial\zeta\partial\tau} + \frac{\partial^4}{\partial\zeta^4}\right)f_2 = -\frac{1}{2}\hat{B}(f_1\cdot f_1), \tag{32b}$$

$$\left(\frac{\partial^2}{\partial\zeta\partial\tau} + \frac{\partial^4}{\partial\zeta^4}\right)f_3 = -\hat{B}(f_1\cdot f_2), \tag{32c}$$

$$\left(\frac{\partial^2}{\partial\zeta\partial\tau} + \frac{\partial^4}{\partial\zeta^4}\right)f_4 = -\frac{1}{2}\hat{B}(f_1\cdot f_3 + f_3\cdot f_1 + f_2\cdot f_2). \tag{32d}$$

Here, $f_1(\zeta,\tau)$ is assumed to be

$$f_1(\zeta,\tau) = \sum_{i=1}^{N}\exp(\vartheta_i), \tag{33}$$

where $\vartheta_i = k_i\zeta + \omega_i\tau$, k_i is the wave number and ω_i is the frequency. Substituting Eq. (33) into Eq. (32a) we have $\omega_i = -k_i^3$.

4.1. Two-soliton Solutions

To determine the two-soliton solutions of Eq. (25), we choose $N = 2$ in Eq. (33), and then $f_1(\zeta,\tau) = \exp(\vartheta_1) + \exp(\vartheta_2)$ with $\vartheta_i = k_i\zeta + \omega_i\tau + \delta_i^{(0)}$, $\delta_i^{(0)}$ is a constant represents the initial phases of solitons, $i = 1, 2$. Substituting $f_1(\zeta,\tau)$ into equation (32b) we have

$$\left(\frac{\partial^2}{\partial\zeta\partial\tau} + \frac{\partial^4}{\partial\zeta^4}\right) f_2 = 3k_1k_2(k_1 - k_2)^2 \exp(\vartheta_1 + \vartheta_2). \tag{34}$$

Therefore, we assume $f_2 = a_{12}\exp(\vartheta_1 + \vartheta_2)$ is a solution of Eq. (34) where a_{12} is a coupling constant yet to be determined. Substituting this formula (i.e., f_2) into Eq. (34), and solved for the coupling constant a_{12} in the terms of wave numbers k_1 and k_2, we get

$$a_{12} = \frac{(k_1 - k_2)^2}{(k_1 + k_2)^2}, \tag{35}$$

which is determines the phase shifts of the respective solitons after overtaking collision (note that $k_1 \neq k_2$). Now we substitute the solutions of f_1 and f_2 into Eq. (32d) we see that, $f_3 = 0$. Thus, without loss of generality we have set $\varepsilon = 1$, the perturbation series expansion (27) becomes

$$F(\zeta,\tau) = 1 + \exp(\vartheta_1) + \exp(\vartheta_2) + a_{12}\exp(\vartheta_1 + \vartheta_2), \tag{36}$$

which is the two-soliton bilinear solution for the stander KdV equation (25). Now, Substituting Eq. (36) into Eq. (26), the two soliton solution of the standard KdV equation (25) is given by

$$\psi = \frac{2}{[1 + e^{\vartheta_1} + e^{\vartheta_2} + a_{12}e^{(\vartheta_1+\vartheta_2)}]^2}\Big[k_1^2e^{\vartheta_1} + k_2^2e^{\vartheta_2} + a_{12}\big(k_2^2e^{\vartheta_1} + k_1^2e^{\vartheta_2}\big)e^{(\vartheta_1+\vartheta_2)} + 2(k_1 - k_2)^2e^{(\vartheta_1+\vartheta_2)}\Big]. \tag{37}$$

Hence, the two-soliton solution of the KdV equation (24) is given by

$$\phi^{(1)} = \frac{12\,B^{\frac{1}{3}}}{A[1 + e^{\theta_1} + e^{\theta_2} + a_{12}e^{(\theta_1+\theta_2)}]^2}\Big[k_1^2e^{\theta_1} + k_2^2e^{\theta_2} + a_{12}\big(k_2^2e^{\theta_1} + k_1^2e^{\theta_2}\big)e^{(\theta_1+\theta_2)} + 2(k_1 - k_2)^2e^{(\theta_1+\theta_2)}\Big], \tag{38}$$

where $\theta_i = k_iB^{-\frac{1}{3}}\xi - k_i^3\tau + \delta_i^{(0)}$, $i = 1, 2$. Thus, for KdV equation (24), Eq. (26) can be rewritten as

$$\phi^{(1)}(\xi,\tau) = \frac{12B}{A}\frac{\partial^2}{\partial\xi^2}\ln f(\xi,\tau), \tag{39}$$

where $f(\xi,\tau)$ for two-soliton solution is given by

$$f(\xi,\tau) = 1 + \exp(\theta_1) + \exp(\theta_2) + a_{12}\exp(\theta_1 + \theta_2), \tag{40}$$

which represents the solution of the two-soliton bilinear form of the KdV equation (24) where $\theta_1 = k_1B^{-\frac{1}{3}}\xi - k_1^3\tau + \delta_1^{(0)}$, and $\theta_2 = k_2B^{-\frac{1}{3}}\xi - k_2^3\tau + \delta_2^{(0)}$. We note that the two-soliton KdV solution (24) can be represented in a number of equivalent forms emphasizing different aspects of the soliton interaction dynamics.

4.2. Three-soliton Solutions

To obtain the three-soliton solutions of the KdV equation, we follow the same way as above by setting $N = 3$ in Eq. (33) to get $f_1 = \exp(\vartheta_1) + \exp(\vartheta_2) + \exp(\vartheta_3)$, and after algebraical calculations, the three-soliton bilinear solutions for the standerd KdV equation (25) is:

$$F(\zeta,\tau) = 1 + e^{\vartheta_1} + e^{\vartheta_2} + e^{\vartheta_3} + b_{12}e^{(\vartheta_1+\vartheta_2)} + b_{13}e^{(\vartheta_1+\vartheta_3)} + b_{23}e^{(\vartheta_2+\vartheta_3)} + b_{123}e^{(\vartheta_1+\vartheta_2+\vartheta_3)}, \tag{41}$$

where the coefficients b_{12}, b_{13}, b_{23} and b_{123} are given by

$$b_{12} = \frac{(k_1 - k_2)^2}{(k_1 + k_2)^2}, \quad b_{13} = \frac{(k_1 - k_3)^2}{(k_3 + k_3)^2}, \quad b_{23} = \frac{(k_2 - k_3)^2}{(k_2 + k_3)^2},$$

and

$$b_{123} = b_{12} b_{13} b_{23} = \frac{(k_1 - k_2)^2 (k_1 - k_3)^2 (k_2 - k_3)^2}{(k_1 + k_2)^2 (k_1 + k_3)^2 (k_2 + k_3)^2}.$$

Therefore, the three-soliton solutions of the KdV equation (24) can be written in the form

$$\phi^{(1)}(\xi,\tau) = \frac{12B}{A} \frac{\partial^2}{\partial \xi^2} \ln g(\xi,\tau), \tag{42}$$

where the function $g(\xi,\tau)$ is obtained as

$$g(\xi,\tau) = 1 + e^{\theta_1} + e^{\theta_2} + e^{\theta_3} + b_{12} e^{(\theta_1+\theta_2)} + b_{13} e^{(\theta_1+\theta_3)} + b_{23} e^{(\theta_2+\theta_3)} + b_{123} e^{(\theta_1+\theta_2+\theta_3)}. \tag{43}$$

where $\theta_i = k_i B^{-\frac{1}{3}} \xi - k_i^3 \tau + \delta_i^{(0)}, i = 1, 2, 3.$

5. Behavior of Soliton Collisions and Phase Shifts

It is noted that there is no amplitude (or velocity) change upon multi-soliton interactions associated with the KdV equation. In other words the interaction is elastic and the only effect of the interaction is a phase shift. In this section we study the behavior of the two solitons interactions of the KdV equation when $\tau \to \pm\infty$, and we derive the formula for the phase shift of the fast-moving and slow-moving soliton, and hence we are generalized this idea on three-soliton interactions.

Now, to obtain the phase shifts due to the interaction of the two-soliton, we introduce the transformation, $\chi_l = B^{-\frac{1}{3}} \xi - k_l^2 \tau$. Then, θ_i can be rewritten in terms of (χ_l, τ) as

$$\theta_i = k_i [\chi_l - (k_i^2 - k_l^2)\tau] + \delta_i^{(0)}, \qquad i = 1,2 \tag{44}$$

If we consider that $k_2 > k_1 > 0$, and $l = 1$ in Eq. (44), we get

$$\begin{aligned} \theta_1 &= k_1 \chi_1 + \delta_1^{(0)}, \\ \theta_2 &= k_2 [\chi_1 - (k_2^2 - k_1^2)\tau] + \delta_2^{(0)}, \end{aligned} \tag{45}$$

where we note that $(k_2^2 - k_1^2) > 0$. The frame of the first (slow) soliton, in which χ_1 is fixed, and θ_1 remains finite, we take the limits cases as $\tau \to \pm\infty$.

Whenever $\tau \to -\infty$, $\theta_2 \to +\infty$, and therefore Eq. (40) leads to

$$f(\xi,\tau) \approx \exp(\theta_2)[1 + \exp(\theta_1 + \ln a_{12})]. \tag{46}$$

Substituting Eq. (46) into Eq. (39), carrying out some algebraic calculations, the solution of Eq. (24) is given by

$$\phi^{(1)} \approx \frac{12B^{\frac{1}{3}}}{A} \frac{k_1^2 e^{\theta_1 + \ln a_{12}}}{(1 + e^{\theta_1 + \ln a_{12}})^2} = \frac{3B^{\frac{1}{3}} k_1^2}{A} \operatorname{sech}^2 \left[\frac{1}{2}(\theta_1 + \ln a_{12})\right], \tag{47}$$

where we put $a_{12} = e^{\ln a_{12}}$ in the Eq. (46), and using the identity $\operatorname{sech}^2(x/2) = 4e^x/(1+e^x)^2$ in the Eq. (47). However, it is appropriate to re-write Eq. (47) in the form

$$\phi^{(1)} \approx \phi_{01} \operatorname{sech}^2 \left[\frac{k_1}{2B^{\frac{1}{3}}} \left(\xi - B^{\frac{1}{3}} k_1^2 \tau + \Delta_-\right)\right], \tag{48}$$

where $\phi_{01} \left(= 3B^{\frac{1}{3}} k_1^2 / A\right)$ is the amplitude of the first (slow) soliton and $\Delta_- = B^{\frac{1}{3}} \ln a_{12} / k_1$ is the phase change of it.

Now, we consider the case when $\tau \to +\infty$. In this case, we have $\theta_2 \to -\infty$, and hence $e^{\theta_2} \to 0$. Therefore Eq. (40) converts to

$$f(\xi,\tau) \approx 1 + \exp(\theta_1). \tag{49}$$

Similarly, using this formula in Eq. (39) we have by direct calculation

$$\phi^{(1)} \approx \phi_{01}\mathrm{sech}^2\left[\frac{k_1}{2B^{\frac{1}{3}}}\left(\xi - B^{\frac{1}{3}}k_1^2\tau\right)\right]. \tag{50}$$

From Eqs. (48) and (50) we see that, after the collision of the two-soliton, the asymptotic trajectory of the slow soliton is shifted backward by a phase shift equal to

$$\Delta_1 = 0 - \Delta_- = -2\frac{B^{1/3}}{k_1}\ln\left|\frac{k_1 - k_2}{k_1 + k_2}\right|, \tag{51}$$

where the minus sign indicates the backward shift.

On the other hand, to obtain the phase shift of the second (fast) soliton after collision with first (slow) soliton, we choose $l = 2$, then from Eq. (44) we get

$$\begin{gathered}\theta_1 = k_1[\chi_2 + (k_2^2 - k_1^2)\tau] + \delta_1^{(0)},\ \ k_2 > k_1 > 0\,, \\ \theta_2 = k_2\chi_2 + \delta_2^{(0)}.\end{gathered} \tag{52}$$

Similarly, in the frame of the fast (second) soliton, we take the limits as $\tau \to \pm\infty$ where χ_2 fixed, and θ_2 remains finite. Then as $\tau \to -\infty$, $\theta_1 \to -\infty$, and from Eq. (40) we have

$$f \approx 1 + \exp(\theta_2), \tag{53}$$

whereas for $\tau \to +\infty$, Eq. (52) gives $\theta_1 \to +\infty$, hence $e^{\theta_1} \to +\infty$. Then, Eq. (40) reduced to

$$f \approx \exp(\theta_1)[1 + \exp(\theta_2 + \ln a_{12})]. \tag{54}$$

Thus from Eq. (39) the two-soliton solution of Eq. (24) is given, in either limit, $\tau \to \pm\infty$, by

$$\phi^{(1)} \approx \phi_{02}\mathrm{sech}^2\left[\frac{k_2}{2B^{\frac{1}{3}}}\left(\xi - B^{\frac{1}{3}}k_2^2\tau + \Delta_\pm\right)\right], \tag{55}$$

where $\phi_{02}\left(= 3B^{\frac{1}{3}}k_2^2/A\right)$ is the amplitude of second soliton and $\Delta_\pm(= \Delta_+,\ \Delta_-)$ is the shift of the trajectory of the second (fast) soliton due to its interaction with the first (slow) soliton. Here, $\Delta_+ = B^{\frac{1}{3}}\ln a_{12}/k_2$ for $\tau \to +\infty$, and $\Delta_- = 0$ for $\tau \to -\infty$. From the above formulae we see that the asymptotic trajectory of the fast soliton is shifted forward by the phase shift

$$\Delta_2 = \Delta_+ - \Delta_- = 2\frac{B^{1/3}}{k_2}\ln\left|\frac{k_1 - k_2}{k_1 + k_2}\right|. \tag{56}$$

It is seen that the phase shifts Δ_1, and Δ_2 are of opposite signs and both of them are proportional to $B^{\frac{1}{3}}$; subsequently the phase shifts will also depend on the dusty plasma parameters.

For the three-soliton interactions, it is easy to see that the phase shift of the first soliton (i=1) due to the other solitons is defined by

$$\delta_1 = -2\frac{B^{1/3}}{k_1}\ln\left|\left(\frac{k_1 - k_2}{k_1 + k_2}\right)\left(\frac{k_1 - k_3}{k_1 + k_3}\right)\right|, \tag{57}$$

and the phase shifts of the second and third solitons respectively are given by

$$\delta_2 = 2\frac{B^{1/3}}{k_2}\ln\left|\left(\frac{k_2-k_3}{k_2+k_3}\right)\right| - \ln\left|\left(\frac{k_1-k_2}{k_1+k_2}\right)\right|, \tag{58}$$

$$\delta_3 = 2\frac{B^{1/3}}{k_3}\ln\left|\left(\frac{k_1-k_3}{k_1+k_3}\right)\left(\frac{k_2-k_3}{k_2+k_3}\right)\right|, \tag{59}$$

where $k_3 > k_2 > k_1 > 0$. It is clear that the phase shifts are functions of the dispersion coefficient (B) and consequently function of the polarization parameter as well as other plasma parameters.

6. Results and Discussion

The propagation and interaction of the DA solitons in an unmagnetized collisionless dusty plasma containing inertial negatively as well as positively charged dust cold, and thermal ions and electrons are investigated. The reductive perturbation technique is employed in order to derive the KdV equation which is appropriate for describing the DA solitons propagation. The Hirota bilinear method is used to study the overtaking collision of multi-soliton solutions. Figure 1 shows the time evaluation of the interaction between two compressive DA solitons ($\phi^{(1)}$ vs ξ) moving in the same direction from left to right with the faster (taller) soliton overtaking the slower (shorter) soliton. It is observed that, at the initial time $\tau = -6$, the faster (taller) soliton with large amplitude is located behind the slower (shorter) one (which has the smaller amplitude). As we evolve in time, the taller soliton will catch up the shorter one and they collide with each other. For $\tau = 0$, the two solitons merge together into a single hump profile (become a single soliton) with amplitude is equal to the difference between the amplitudes of the two solitons before its interaction. After finite time, a large soliton overtakes a small one and after time $\tau = 6$, they regain their original shapes. The only noticeable change due to the interaction of the two solitons is a phase shift from where the wave would have been if there was no interaction.

The combined profile of the compressive two-soliton interaction is presented in Figs. 2(a) and 2(b) where Fig. 2(a) is plotted without polarization force effect (i.e., when $R = 0$) while Fig. 2(b) is plotted with polarization force. From these figures, we can see that there is a shift in the solitons due to an elastic collision and the nonlinear interaction, this shift is called the phase shift. The phase shift is particularly large for the small amplitude soliton. The larger amplitude soliton shifted forward whereas the smaller one shifted backward due to the collision. It is also observed that, the polarization force leads to reduce the amplitudes of both larger and smaller solitons.

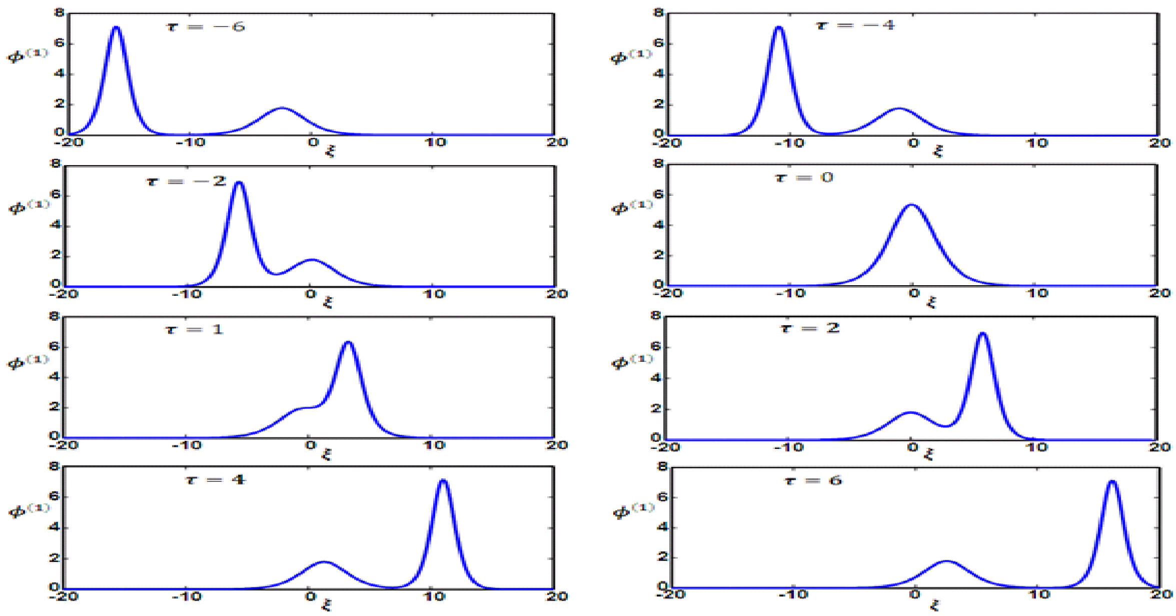

Figure 1: Compressive two-soliton profile for various τ, with $Z = 0.2$, $k_1 = 0.8$, $k_2 = 1.6$, $R = 0.5$, $\mu_i = 0.6$, $\mu_e = 0.3$, $\sigma_i = 0.3$, and $\mu = 5$.

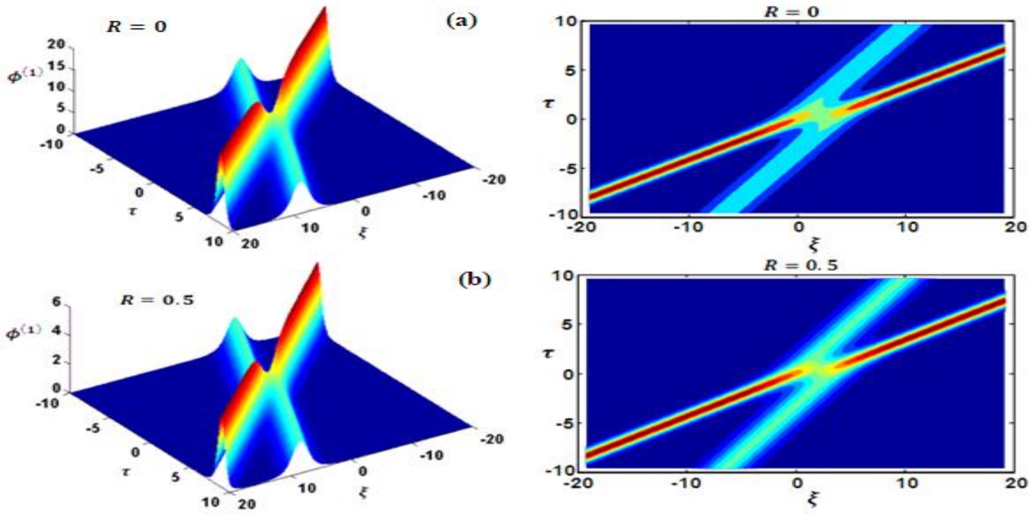

Figure 2: The interaction profile of the compressive two-solitons and its contour plots. (a) without polarization force effect ($R = 0$), and (b) with polarization force effect ($R = 0.5$) and for $Z = 0.2$, $k_1 = 1$, $k_2 = 1.5$, $\mu_i = 0.7$, $\mu_e = 0.3$, $\sigma_i = 0.2$, and $\mu = 5$.

To clarify more, Fig. 3 shows a plot of the superimposition of the lines of the asymptotic trajectories of the slow and fast solitons on the contour plot of the two-soliton solutions. It is found that the asymptotic trajectory of the slow-moving soliton is shifted backward by a phase shift equals to $-2\sqrt[3]{B}\ln|\sqrt{a_{12}}|/k_1$ (the minus sign indicates the backward shift.), and the asymptotic trajectory of the fast-moving soliton is shifted forward by a phase shift equals to $2\sqrt[3]{B}\ln|\sqrt{a_{12}}|/k_2$. The line of asymptotic trajectories passes through the middle of the slow and fast moving solitons both in the infinite past and future in time, which shows that the analytic computation is correct. Comparison of Fig. 3(a) and Fig. 3(b) demonstrates that the polarization force has a significant effect on the phase shift and the asymptotic trajectories of both solitons.

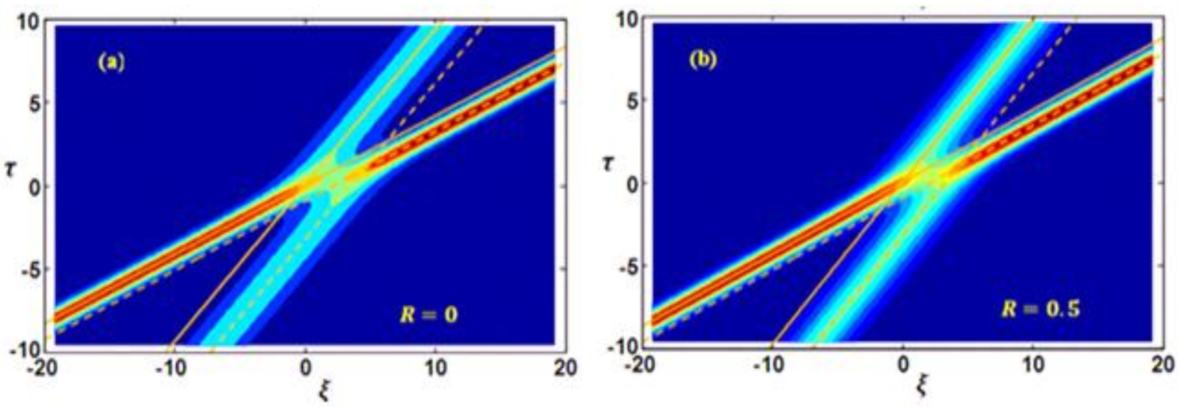

Figure 3: Superimposition of the trajectories on contour plot of the compressive two-soliton. (a) Without polarization force effect ($R = 0$). and (b) with polarization force effect ($R = 0.5$) and for $Z = 0.2$, $k_1 = 1$, $k_2 = 1.5$, $\mu_i = 0.7$, $\mu_e = 0.3$, $\sigma_i = 0.2$, and $\mu = 5$.

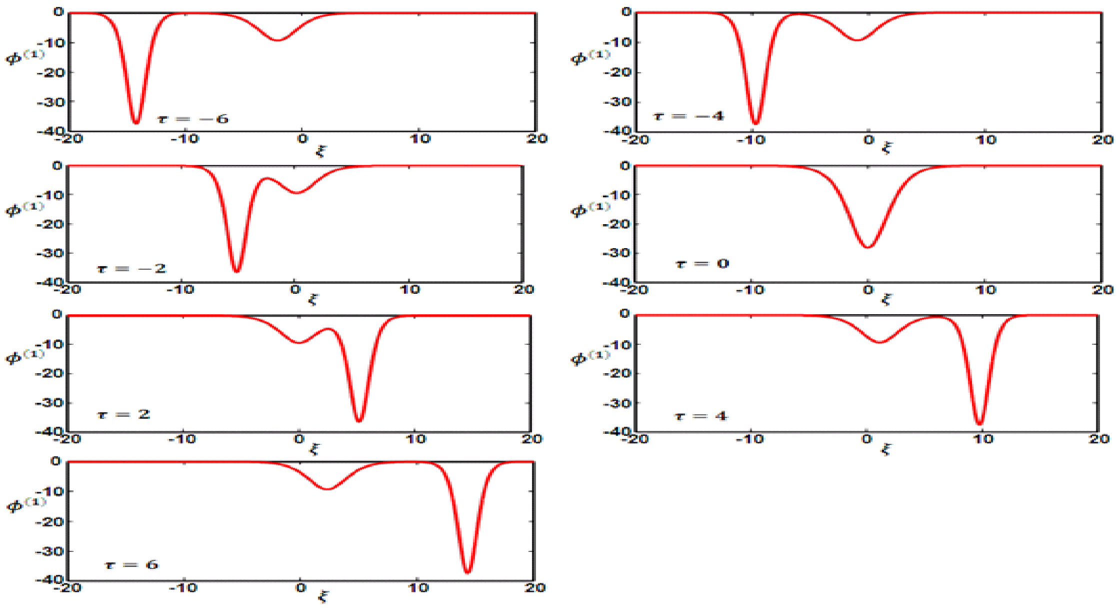

Figure 4: Rarefactive two-soliton profile for different values of τ, with $Z = 0.02$, and with same values of other parameters as Fig. 1.

On the other hand, the time evaluation of the interaction of rarefactive two solitons is displayed in Fig. 4 when $Z = 0.01$. Similarly, we can see that at $\tau = -6$, the taller soliton is behind the smaller one, and when $\tau = -2$, the taller soliton is getting closer to the shorter one. The two solitons merge and become one soliton at $\tau = 0$. But after certain time $\tau = 2$, they separate from each other, and then finally they depart from each other when $\tau = 6$.

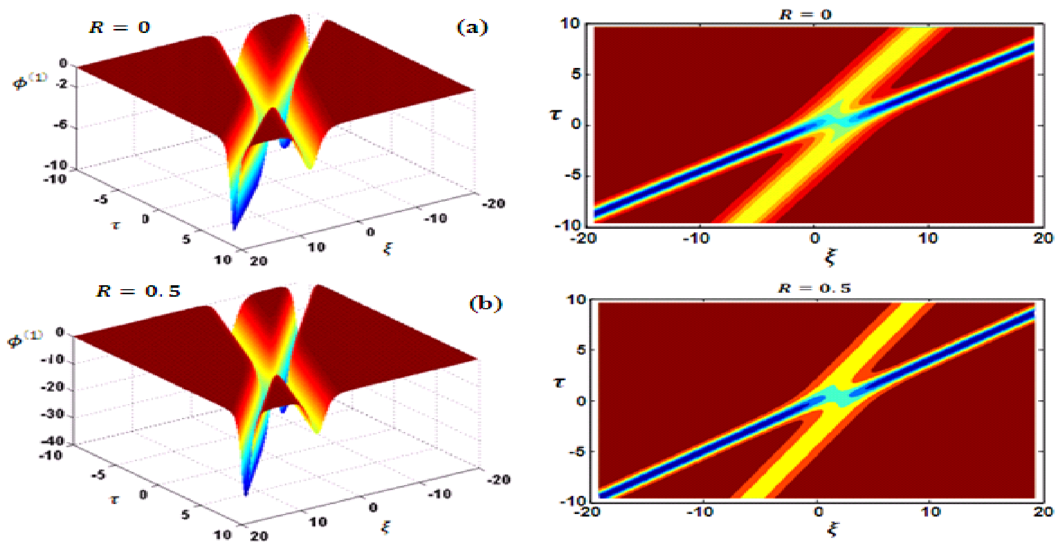

Figure 5: The interaction profile of the compressive two-solitons and its contour plots. (a) without polarization force effect ($R = 0$), and (b) with polarization force effect ($R = 0.5$) and for $Z = 0.2$, $k_1 = 1$, $k_2 = 1.5$, $\mu_i = 0.7$, $\mu_e = 0.3$, $\sigma_i = 0.2$, and $\mu = 5$.

The combined profile of the rarefactive two-soliton collision is presented in Figs. 5 (a) and 5 (b) without and with polarization force effect, respectively. As it clear from these figures, the smaller soliton is retarded in time whereas the larger one is pushed forward. Figure 5(b) depicts that the presence of the polarization force leads to an increase in the amplitudes of both larger and smaller solitons. Clearly, the modification in the phase shift due to the presence of the polarization force is also visible in Fig. 5(b). Also, Figs 6(a) and 6(b) show a plot of the superimposition of the lines of the asymptotic trajectories of the slow soliton and fast soliton on the contour plot of the rarefactive two-soliton collision in the absence of the polarization force [Fig. 6(a)] and in the presence of the polarization force [Fig. 6(b)]. From these figures, we can also see that the line of asymptotic trajectories passes through the middle of the slow and fast moving solitons both in the infinite past and future in time. It is found also from figure 6 that, the asymptotic trajectory of the slow soliton is shifted backward by a phase shift equals to $-2\sqrt[3]{B}\ln|\sqrt{a_{12}}|/k_1$, and the asymptotic trajectory of the fast soliton is shifted forward by a phase shift equals to $2\sqrt[3]{B}\ln|\sqrt{a_{12}}|/k_2$. Due to the presence of the polarization force, the lines of asymptotic trajectories of two solitons are shifted.

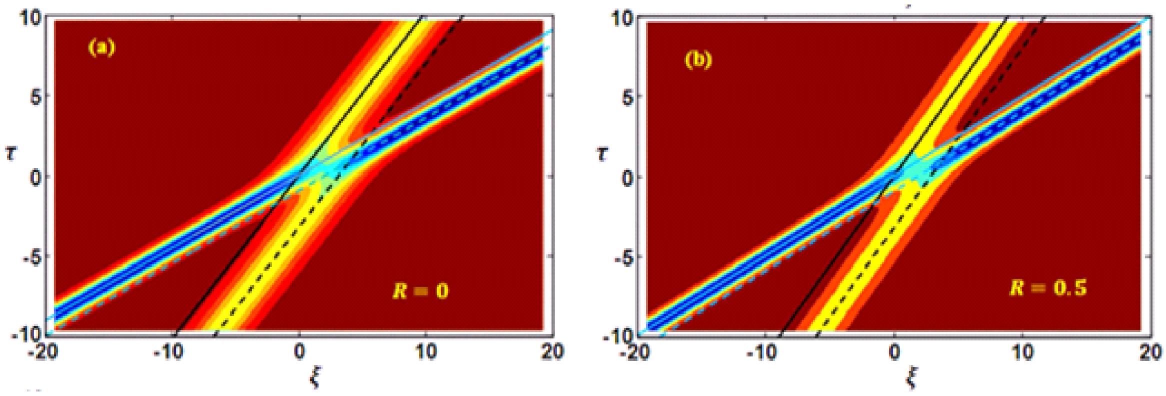

Figure 6: Superimposition of the asymptotic trajectories on contour plot of the rarefactive two-soliton. (a) without polarization force effect, and (b) with polarization force effect and for $Z = 0.01$, $k_1 = 1$, $k_2 = 1.5$, $\mu_i = 0.6$, $\mu_e = 0.3$, $\sigma_i = 0.2$, and $\mu = 5$.

In Figs. 7 and.8, the time evolution of the interaction of both compressive and rarefactive three-soliton profile respectively have been plotted with the plasma parameters: $k_1 = 1$, $k_2 = 1.5$, $k_3 = 2$, $R = 0.6$, $\mu_i = 0.7$, $\mu_e = 0.3$, $\sigma_i = 0.2$, and $\mu = 5$. From these figures, we have shown that for $\tau = -4$ larger amplitude soliton is behind all other small amplitude solitons. When $\tau = -2$, the three solitons merge and become one soliton at $\tau = 0$. But, at $\tau = 2$, they separate from each other, and then finally they depart from each other when $\tau = 4$.

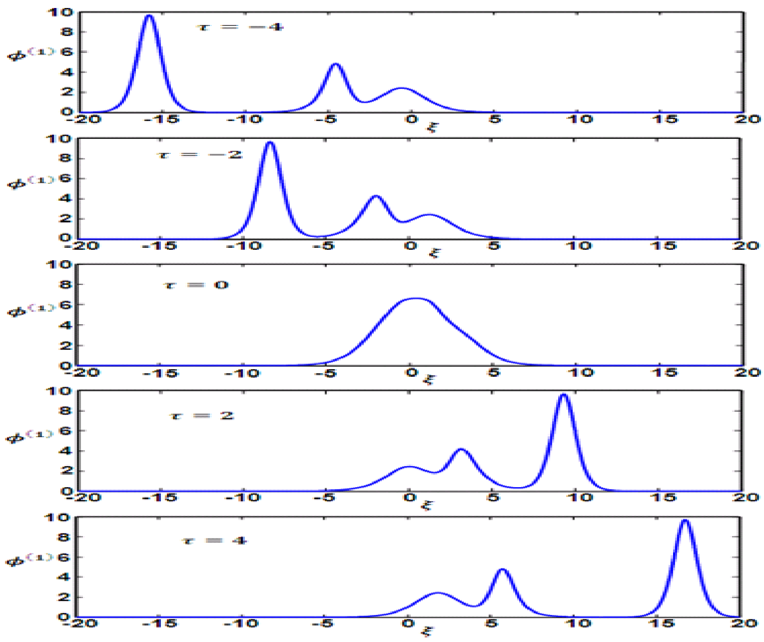

Figure 7: Compressive three-soliton profile for various τ, with $k_1 = 1$, $k_2 = 1.5$, $k_3 = 2$, $R = 0.6$, and other parameters same as Fig. 1.

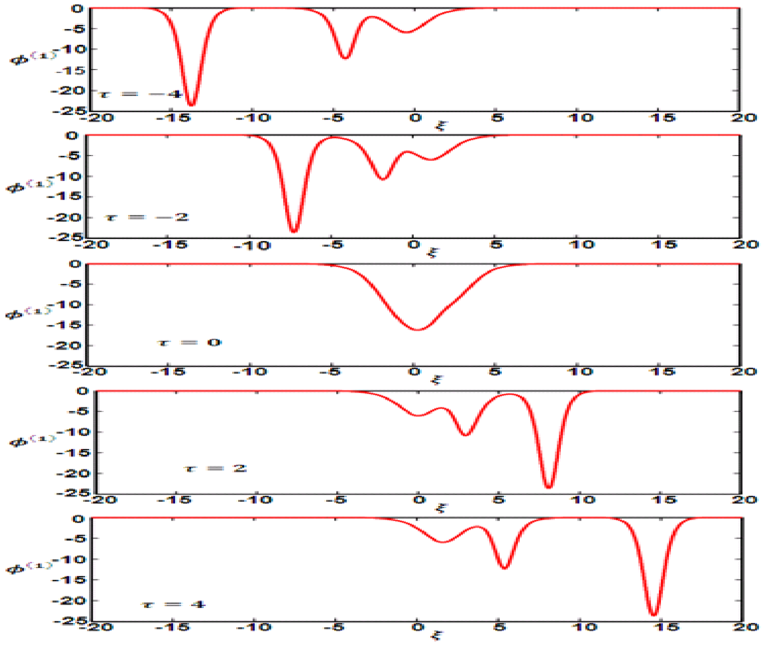

Figure 8: Rarefactive three-soliton profile for different values of τ, with $Z = 0.01$. The other parameters as in Fig.1.

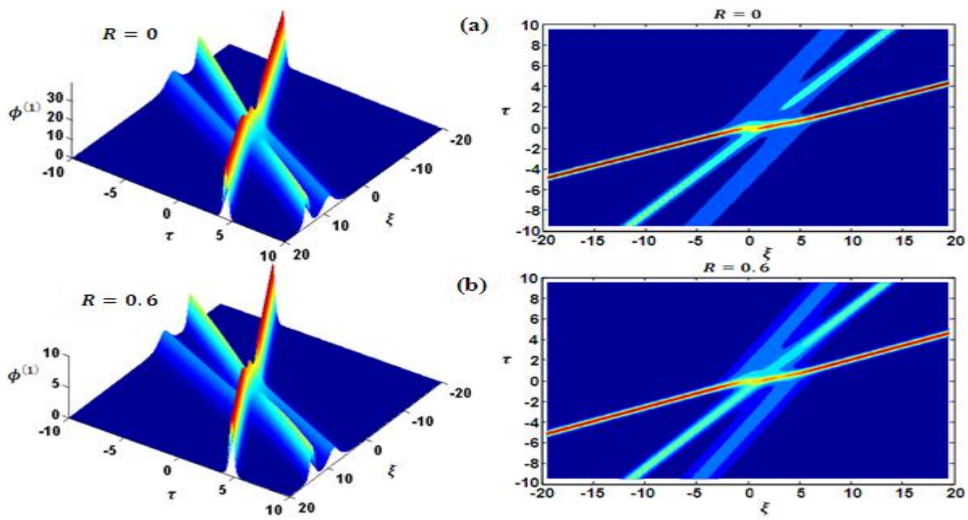

Figure 9: The interaction profile of the compressive three-solitons and its contour plots. (a) without polarization force effect ($R = 0$), and (b) with polarization force effect ($R = 0.6$). Other parameters are taken a $Z = 0.2$, $k_1 = 1$, $k_2 = 1.5$, $\mu_i = 0.7$, $\mu_e = 0.3$, $\sigma_i = 0.2$, and $\mu = 5$.

Figure 9(a) shows an overtaking elastic collisions of three compressive solitons in (ξ, τ) plane with its contour plot when $R = 0$ (i.e., without the polarization force). Figure 9(b) illustrates an overtaking elastic collisions between three-soliton in (ξ, τ) plane with its contour plot at $R = 0.6$ (i.e., when polarization force is considered). In Figs. 9(a) and 9(b), soliton with large amplitude travels faster and catches the smaller one. After the collision, the three solitons remain their original shapes and amplitudes expect for the phase shifts. Furthermore, in the presence of the polarization force, the amplitude of the multi-soliton will decrease as depicted in Fig. 9(b). The phase shift is also visible in Fig. 9 due to the interaction among the three solitons.

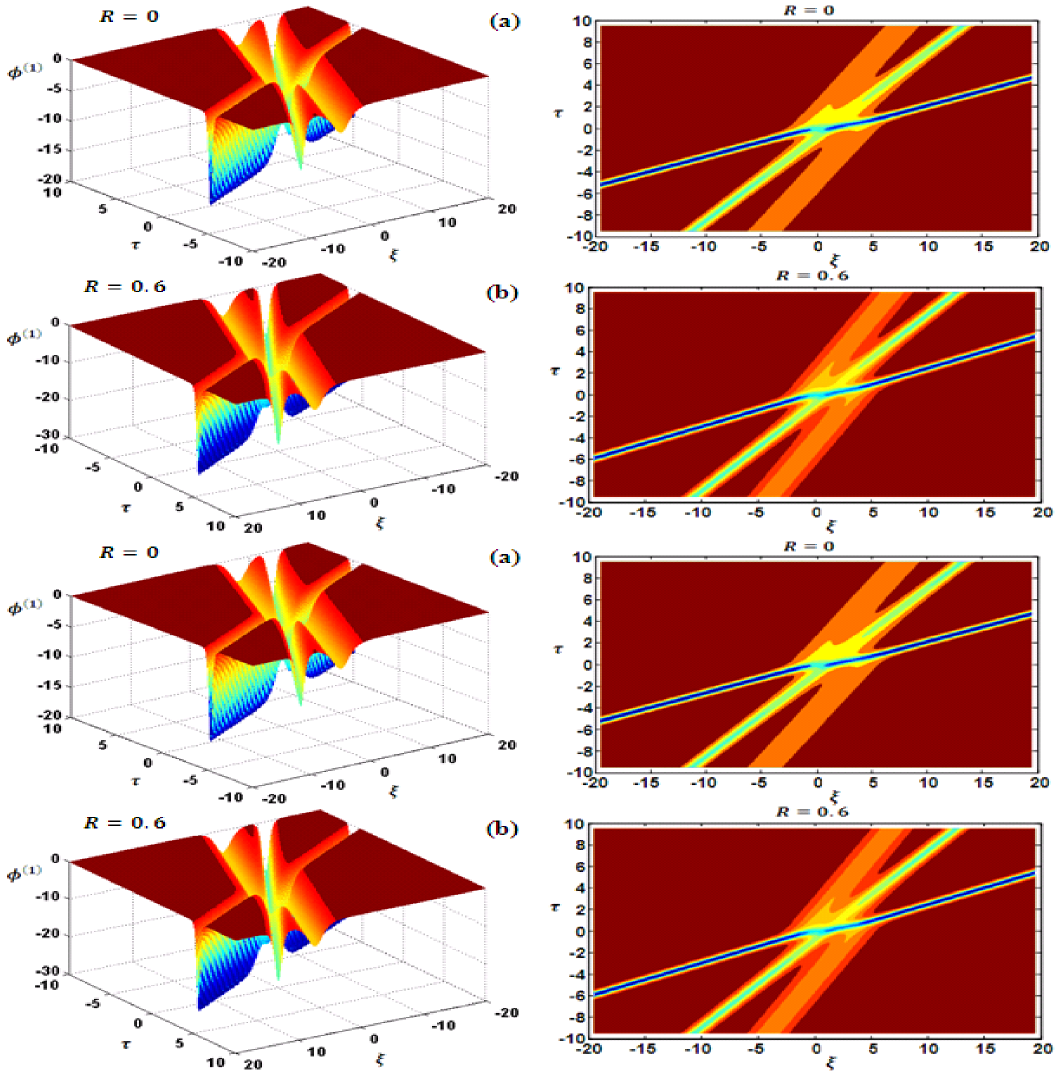

Figure 10: The interaction profile of the rarefactive three-soliton and its contour plots. (a) without polarization force effect ($R = 0$), and (b) with polarization force effect ($R = 0.6$). Other parameters are taken as $Z = 0.01$, $k_1 = 1$, $k_2 = 1.5$, $\mu_i = 0.7$, $\mu_e = 0.3$, $\sigma_i = 0.2$, and $\mu = 5$.

The interaction profile among three rarefactive DA solitons propagates in the same direction with their corresponding contour plots is shown in Fig. 10. One can clearly see that the soliton with larger amplitude has a greater velocity than another with smaller amplitude. Consequently, as time goes on, the larger soliton catches up with the smaller one and the collision occurs and the larger soliton has overtaken the smaller one. From Figs. 10(a) and 10(b), it is noted that the amplitudes of the rarefactive DA solitons in the presence of polarization force [Fig. 10(b)] are larger than those in the absence of the polarization force [Fig. 10(a)]. Furthermore, we find that the change of trajectory for each DA soliton is evident after interaction.

Figure 11 illustrates the variation of phase shift Δ_1 after the interaction of two solitons against polarization force parameter R, for two different values of Z with $k_1 = 1, k_2 = 1.5$, $\sigma_i = 0.3$, $\mu_i = 0.7$, $\mu_e = 0.3$, $\mu = 5$. It is noticed that with an increase in the polarization force parameter R, the phase shift decreases, but it is increasing with the increase of Z. The effect of the polarization force on the phase shift is more pronounced for lower value of Z.

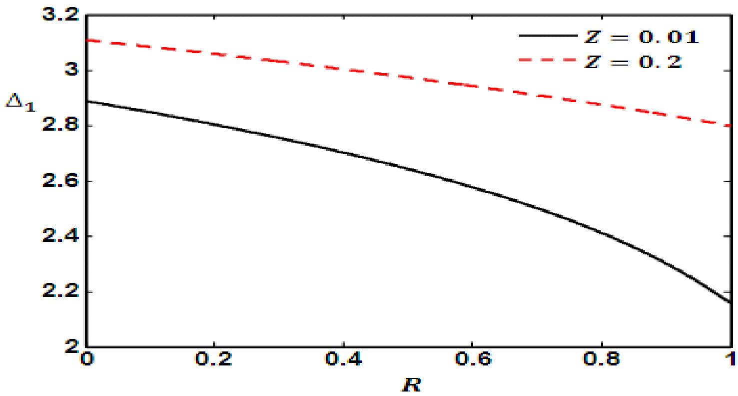

Figure 11: The phase shift (Δ_1) after the overtaking interaction between two DA solitons versus the polarization force parameter R for two different values of Z with $k_1 = 1$, $k_2 = 1.5$, $\sigma_i = 0.3$, $\mu_i = 0.7$, $\mu_e = 0.3$, and $\mu = 5$.

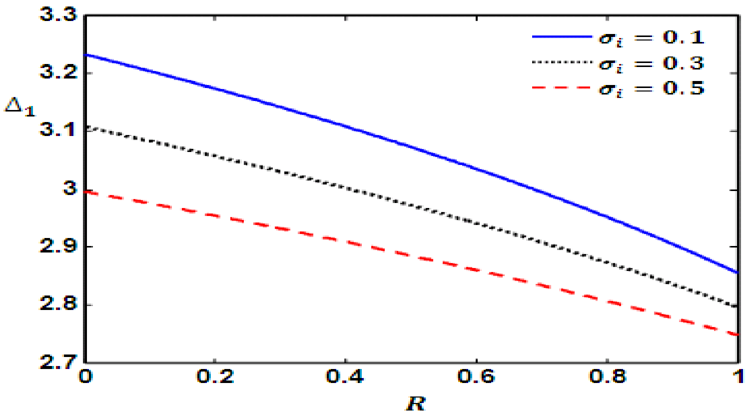

Figure 12: The phase shift (Δ_1) after the overtaking interaction between two DA solitons versus the polarization force for different values of σ_i when Z=0.2. Other parameters are $k_1 = 1$, $k_2 = 1.5$, $\mu_i = 0.7$, $\mu_e = 0.3$, and $\mu = 5$.

In Figs. 12 and 13, we have presented the variation of phase shift Δ_1 against the polarization parameter R with different values of the ion-to-electron temperature ratio σ_i in the cases of $Z = 0.2$ and $Z = 0.01$, respectively. As shown in Fig. 12, in the case of $Z = 0.2$, an increase of both the polarization parameter R and σ_i, decreases the phase shift Δ_1. However, in the case of $Z = 0.01$, Fig. 4 indicates that, within the range of $R < 0.8$, the phase shift Δ_1 decreases as both of the polarization parameter R and the ion temperature ratio σ_i increase, but in the range of $R > 0.8$, the phase shift increases with the increase of σ_i. This means that the influence of the polarization force decreases with increasing ion temperature. Figure 14 shows the dependence of the phase shift on both of the electron-to-ion density ratio ρ and positive-to-negative dust ratio μ. It turns out that the phase shift Δ_1 decreases as the ion density ρ increases. But Δ_1 increases with the increase of μ.

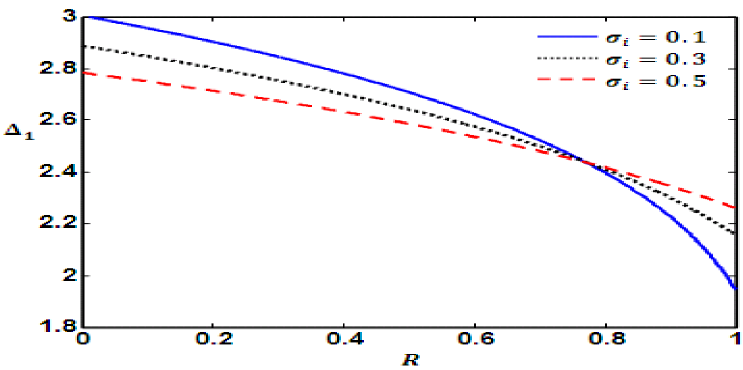

Figure 13: The phase shift (Δ_1) after the overtaking interaction between two DA solitons versus the polarization force for different values of σ_i when Z=0.01. The other parameters as in Fig. 11.

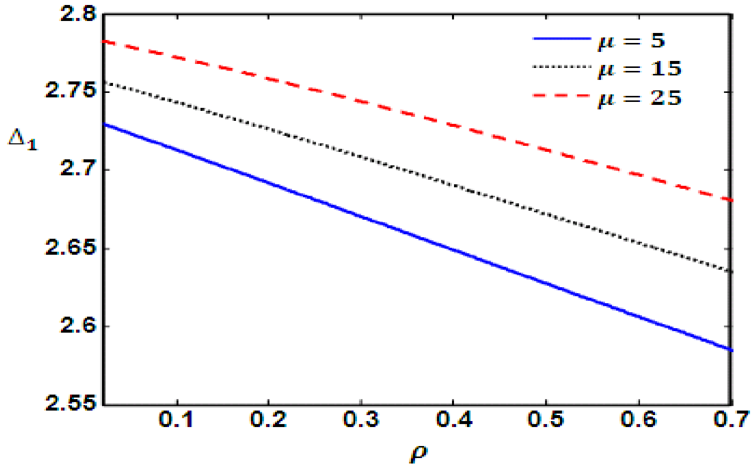

Figure 14: The phase shift (Δ_1) after the overtaking interaction between two DA solitons versus ρ for different values of μ with $k_1 = 1$, $k_2 = 1.5$, $\sigma_i = 0.3$, $\mu_i = 0.7$, and Z=0.01.

Figure 15 indicates the variation of the phase shift δ_1 with R for different values of Z after the overtaking interaction between three solitons with $k_1 = 1, k_2 = 1.5$, $k_3 = 2$, $\sigma_i = 0.2$, $\mu_i = 0.7$, $\mu_e = 0.3$, and μ =5**.** As depicted in Fig. 14, the phase shift δ_1 increases with the increase of Z, but it decreases with the increase in R.

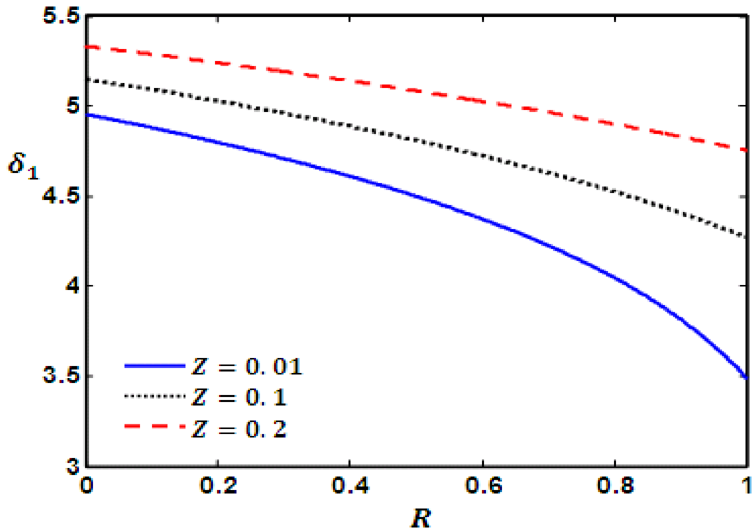

Figure 15: The phase shift (δ_1) after the overtaking interaction between three DA solitons versus the polarization force for different values of Z with $k_1 = 1$, $k_2 = 1.5$, $k_3 = 2$, $\sigma_i = 0.2$, $\mu_i = 0.7$, $\mu_e = 0.3$, and μ =5.

7. Conclusion

In this paper, we have studied the nature of the nonlinear propagation and interaction of two-soliton and three-soliton solutions of the KdV equation (24) in an opposite polarity dusty plasma consisting of negatively and positively charged cold dust fluids, Boltzmann velocity distributed electrons and ions, including the generalized polarization force. The KdV equation (24) is transformed into a standard KdV equation (25) by using a suitable transformation. By using the Hirota's bilinear method, the two-and three-soliton solutions for the KdV equation (24) have been successfully obtained. Both compressive and rarefactive solitons are found to exist in the dusty plasma. The large value of Z is found to yield compressive solitons and smaller Z is found to yield rarefactive solitons. Plots of the solutions were made and it was shown that the solitons interact and keep their forms after collision with one another. It has been observed that the soliton with large amplitude travels faster and catches the smaller one. After the overtaking collision, the solitons retain their original shapes and amplitudes expect for the phase shifts. It was observed that the larger amplitude soliton shifted forward while that of the smaller amplitude shifted backward as a result of the phase shift.

It has been found that, the phase shifts are significantly affected by the polarization force parameter R, number charge ratio Z, ion-to-electron temperature ratio σ_i, positive-to-negative dust mass ratio μ, and the ratio of the densities of electrons to ions ρ. Finally, it is observed that the polarization force gives a higher amplitude in the case of rarefactive solitons and gives a smaller amplitude in the case of compressive solitons.

References

[1] E. C. Whipple, T. G. Northrop, and D. A. Mendis, *J. Geophys. Res*. **90**, 7405 (1985).
[2] C. K. Goertz, *Rev. Geophys*. **27**, 271 (1989).
[3] G. E. Cliolek and T. Ch. Mouschovias, *Astrophys. J*. **418**, 774 (1993).
[4] F. Verheest, *Space Sci. Rev*. **77**, 267 (1996).
[5] P. K. Shukla and A. A. Mamun, "Introduction to dusty plasma physics" (Institute of Physics Publishing Ltd., Bristol, 2002).
[6] P.K. Shukla and V.P. Silin, *Phys. Scr*. **45**, 508 (1992).
[7] N. N. Rao, P. K. Shukla, and M. Y. Yu, *Planet. Space Sci*. **38**, 543 (1990).
[8] A. Barkan, R. Merlino, and N. D'Angelo, *Phys. Plasmas* **2**, 3563 (1995).
[9] S. Hamaguchi and R. T. Farouki, *Phys. Rev*. E **49**, 4430 (1994).
[10] S. Hamaguchi and R. T. Farouki, *Phys. Plasmas* **1**, 2110 (1994).
[11] S. A. Khrapak, A. V. Ivlev, V. V. Yaroshenko and G. E. Morfill, *Phys. Rev. Lett*. **102**, 245004 (2009).
[12] P. Bandyopadhyay, U. Konopka, S. A. Kharapak, G. E. Morfill and A. Sen, *New J. Phys*. **12**, 073002 (2010).
[13] M. Asaduzzaman and A. A. Mamun, *Phys. Plasmas* **19**, 093704 (2012).
[14] S. Pervin, S. S. Duha, M. Aaduzzaman and A. A. Mamun, *J. Plasma Phys*. **79**, 1 (2013).
[15] P. Dutta, P. Das, and P. K. Karmakar, Astrophys. *Space Sci*. **361**, 322 (2016).
[16] S. K. El-Labany, W. F. El-Taibany, and A. M. Abdelghany, *Phys. Plasmas* **25**, 013709 (2018).
[17] O. Havnes, J. Trøim, T. Blix, W. Mortensen, L. I. Naesheim, E. Thrane, and V. Tønnesen, *J. Geophys. Res.* **101**, 10839, https://doi.org/10.1029/96JA00003 (1996).
[18] M. Horanyi, *Annu. Rev. Astron. Astrophys*. **34**, 383 (1996).
[19] T. A. Ellis and J. S. Neff, *Icarus* **91**, 280 (1991).
[20] T. Akhter, M. M. Hossain, and A. A. Mamun, *Phys. Plasmas* **19**, 093707 (2012).
[21] W. F. El-Taibany, E. E. Behery, S. K. El-Labany, and A. M. Abdelghany, *Phys. Plasmas* **26**, 063701 (2019).
[22] J. H. Dinkel, C. Setzer, and K. E. Lonngren, *Chaos Solitons and Fractals*, **12**, 91 (2001).
[23] L. Bringol-Barge and T. W. Hyde, *Adv. Space Res*.**29**, 1283 (2002).
[24] N. J. Zabusky and M. D. Kruskal, *Phys. Rev. Lett*. **15**, 240 (1965).
[25] C. S. Gardner, J. M. Greener, M. D. Kruskal, and R. M. Miura, *Phys. Rev. Lett*. **19**, 1095 (1967).
[26] R. Hirota, *Phys. Rev. Lett*. **27**, 1192 (1971).
[27] K. Roy, T. K. Maji, M. K. Ghorui, P. Chatterjee, and R. Roychoudhury, *Astrophys. Space Sci*. **352**, 151 (2014).
[28] A. Saha and P. Chatterjee, *Astrophys Space Sci*. **353**, 169 (2014).
[29] M. A. H. Khaled, M. A. Shukri, and Y.A.A. Hager, *Phys. Plasmas* **26**, 103702 (2019).
[30] H. Washimi and T. Taniuti, *Phys. Rev. Lett*. **17**, 996 (1966).